Photoinduced Quantum Interference Antiresonances in π-Conjugated Polymers

R. Österbacka,[1] X. M. Jiang,[2] C. P. An,[2] B. Horovitz,[3] and Z. V. Vardeny[2]

[1]Department of Physics, Åbo Akademi University, Porthansgatan 3, FIN-20500 Turku, Finland
[2]Department of Physics, University of Utah, 114 South 1400 East, Salt Lake City, Utah 84112-0830
[3]Department of Physics, Ben Gurion University of the Negev, Beer-Sheva 84105, Israel

We observed photoinduced quantum interference antiresonances between several discrete infrared-active vibrations and the lower-polaron continuous absorption band in a series of π-conjugated polymer films having superior planar orders, where the polaron transition energy is relatively small. The photoinduced Fano-type antiresonances are well explained by extending the amplitude mode model beyond the adiabatic limit. The agreement between the data and the model confirms the presence of a continuous electronic band above the polaron state. We show that high frequency modes are strongly coupled to electrons, with implications for superconductivity.

The rapid development of the quality of π-conjugated polymers (PCP) through better synthesis and innovative polymers has led to many interesting electronic phenomena and applications such as organic light emitting diodes (OLED) with high luminosity [1], two-dimensional delocalization of charge carriers [2,3], high mobility field effect transistors (FET) [4], and very recently also superconductivity at temperature of about 2 K [5]. Yet the existence of a continuum electronic state in the charge manifold of such superior polymers has still remained elusive. So far there exists only one definite experimental example of the existence of a continuum band threshold in PCP, namely the Frantz-Keldysh−type oscillation measured in the electroabsorption spectrum of a polydiacetylene single crystal [6].

In this work we used the technique of photoinduced absorption (PA) in highly ordered PCP to measure the existence of a continuum of electronic states in the charge manifold of ordered polymer films. The planar order in the films increases the polymer chain stiffness, and this leads to a smaller polaron relaxation energy in the films, E_r of order 50 meV; E_r is defined as the gap between the polaron state and the continuum above (Fig. 1, inset) and can be measured via the polaron transition P_1. At these E_r values the photoinduced polaron optical transitions to the adjacent electronic band overlap with a series of photoinduced infrared-active vibrations (IRAV), which are known to be formed in PCP when charges are added to the polymer chains [7]. When these conditions are met, we measured a series of quantum interference antiresonances (AR) between the two types of excitations, namely the discrete IRAV and the polaron PA band. The Fano-type AR can be very well explained by extending the amplitude mode model [7] to a nonadiabatic situation in the presence of a continuous electronic band. We consider the obtained fit between the data and the model calculation as evidence for the existence of a continuum band above the polaron state in the charge manifold of ordered PCP, justifying the semiconductor quantitative treatments that have been done so far in dealing with OLED [1] and organic FET

[4]. Moreover, we found from the detailed fit to the photoinduced polaron spectrum the existence of a high frequency phonon with relatively strong e-p coupling, with clear implications to the recently discovered superconductivity in PCP [5].

For the PA measurements we used a modified Fourier-transform infrared spectrometer equipped with a high sensitivity detector in the range of 500 to 2500 cm^{-1}, which allowed an Ar$^+$ laser beam to excite the PCP film [3]. The films were placed in a low-temperature cryostat in the sample chamber of the spectrometer. We measured alternate transmission spectra, $T(\omega)$ of the film with the laser beam on and off until resolution of 10^{-5} in T was achieved; typically we obtained such a fine resolution when averaging about 20 000 scans. We then obtained
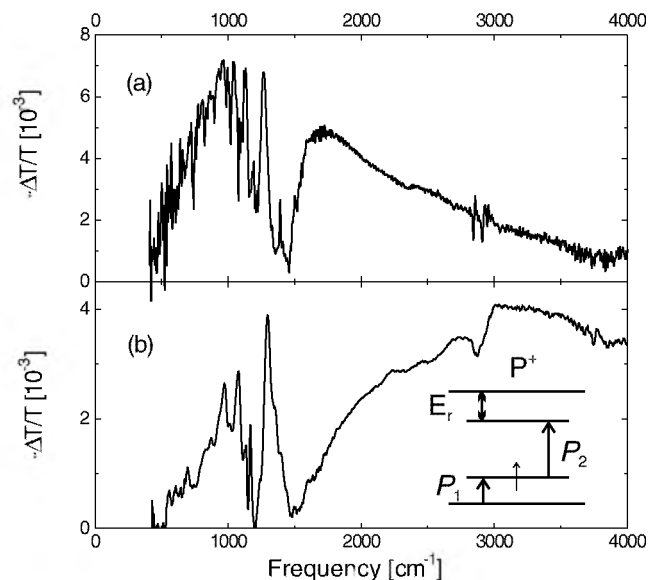

FIG. 1. PA spectra in the mid-IR range for films of RR-P3HT (a) and RR-P3AT with a long attached alkyl side group (b). The inset shows schematically the two polaron levels in the gap and associated optical transitions P_1 and P_2; the polaron relaxation energy E_r is also defined ($E_r \approx P_1$).

the difference spectrum, ΔT between $T(\text{on})$ and $T(\text{off})$, and normalized it by $T(\text{off})$ to obtained the PA, or $\Delta T/T$ spectrum.

The samples were high quality PCP thin films that were spin cast on CsI substrates. The series of ordered PCP films contain the highly planar blue emitting polymers, such as ladder-type methyl substituted poly-p-phenylene (mLPPP) and poly-di octylfluorene (PFO), a di-substituted polyacetylene (PDPA), several regio-regular poly(3 alkyl-thiophene) (RR-P3AT), and a highly ordered poly(phenylene-acetylene) (PPE). The latter two polymer classes are known to form two-dimensional lamellar structures upon spin casting [2].

Figure 1 shows the PA spectra of two RR-P3AT films that were measured at 20 K, a RR-poly(hexyl-thiophene) (P3HT) and another RR-P3AT that has a very long alkyl side group. We note that whereas RR-P3HT forms lamellae in the film [2,3], lamellae are not formed within the second polymer because of the very long attached side group. One of the pronounced differences between the two PA spectra in Fig. 1 is the PA band marked P_1; in RR-P3HT it peaks at about 1000 cm^{-1}, whereas it peaks at about 3000 cm^{-1} in the less ordered polymer film. We therefore conclude that the polaron relaxation energy E_r is substantially smaller in the more ordered film. The sub-linear intensity dependence of the P_1 band points to bimolecular recombination kinetics. The most striking difference between the two PA spectra, however, is the sharp photoinduced features at frequencies below about 1600 cm^{-1} that are due to photoinduced IRAV. Whereas in the less ordered film the photoinduced IRAV appear as positive absorption lines [Fig. 1(b)], they appear as dips or AR superimposed on the P_1 PA band in the more ordered film [Fig. 1(a)]. These AR lines are apparently caused due to the overlap between the IRAV lines and the P_1 band. Moreover, the AR spectrum [Fig. 1(a)] contains sharper lines and consequently is much richer than the IRAV spectrum.

Photoinduced AR lines are not unique to RR-P3HT, as was previously assumed [3]. In fact, we found that AR are quite a generic phenomenon in ordered films, where the polaron P_1 band overlaps with the IRAV. Figures 2(a) to 2(d) show the PA spectra of other ordered polymer films. In all of them photoinduced AR superimposed on P_1 are apparent. In some polymers the separation between IRAV and AR is difficult, especially where the overlap with the P_1 band is less pronounced [Figs. 2(a) to 2(c)]. We note that the literature contains other examples of photoinduced AR in the PA spectra of PCP, such as in polydiacetylene single crystals [8], for example, and other polymer films [9–11] where the AR phenomenon has not been identified or recognized, as well as in charge-induced absorption measurements in RR-P3HT [12].

We analyze the AR spectrum using the amplitude mode (AM) model [7], which has had spectacular success in explaining the resonant Raman scattering (RRS) dispersion,
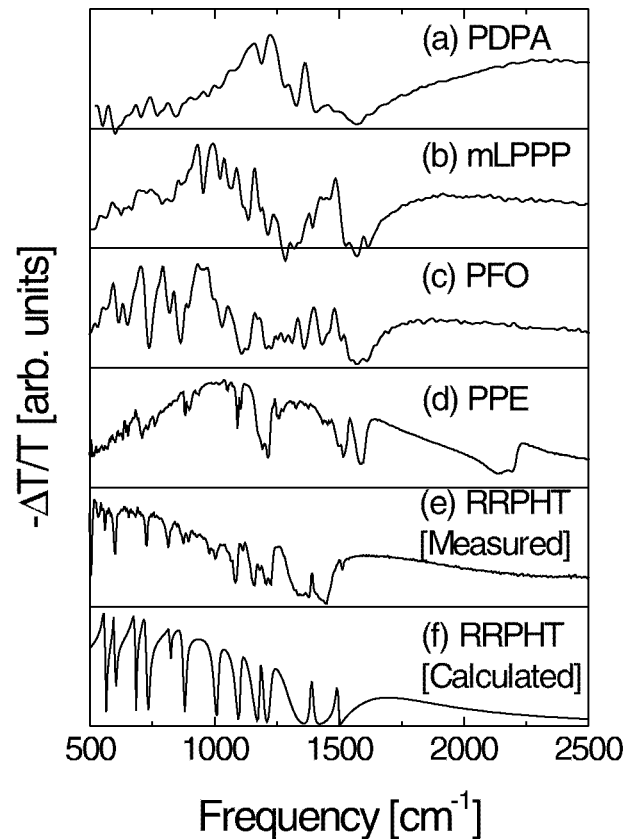

FIG. 2. PA spectra in the mid-IR range for various ordered PCP films. In (f) the calculated spectrum for RR-P3HT is shown (see text), and compared to the data (e).

as well as photoinduced and doping induced IRAV in PCP [13]. In all of these previous applications of the AM model it has been explicitly assumed that the adiabatic approximation holds true [7]. This was a correct assumption since the Raman frequencies are much smaller than the optical gap, and the IRAV frequencies are much smaller than the energy of the photoinduced or doping-induced electronic bands [13]. This approximation, however, does not hold in our case; we thus have to modify the AM model to include nonadiabatic effects.

An important ingredient of the AM model is that all IRAV are interconnected by being coupled to the same electronic dimerization pattern [7,13–15]. This case is unique to AR in polymers, and substantially differs from the more regular Fano-type resonance treatments in other materials [16–20]. Consider a collective center of mass coordinate pinned with strength α [7]. This results in the collective phonon propagator, $D_a(\omega) = D_0(\omega)/[1 - \alpha D_0(\omega)]$, where $D_0(\omega)$ is the bare phonon propagator. The latter is given by [7] $D_0(\omega) = \sum_{n=1}^{N} \frac{\lambda_n}{\lambda} \frac{(\omega_n^0)^2}{\omega^2 - (\omega_n^0)^2 + i\delta_n}$, and ω_n^0, δ_n, and λ_n are the bare phonon frequencies, their natural linewidth (inverse lifetime) and electron-phonon (e-p) coupling constants, with $\sum_n^N \lambda_n = \lambda$, the total e-p coupling. To evaluate the conductivity $\sigma(\omega)$ we consider the random phase approximation (RPA), given regardless

of an adiabatic condition, by the form

$$g(\omega) = \frac{\omega^2}{E_r^2} \frac{-\lambda D_\alpha(\omega)f^2(\omega)}{1 + 2\lambda D_\alpha(\omega)\Pi_\phi(\omega)}, \qquad (1)$$

where $f(\omega)$ is the polaron current coupling to phonons and $\Pi_\phi(\omega)$ is the phonon self-mass correction due to the electron-phonon coupling. These RPA terms contain the sharp structure of $D_\alpha(\omega)$, whereas additional non-RPA terms involving convolutions of $D_\alpha(\omega)$ contribute a smooth background term.

We write $\sigma(\omega)$ in the form

$$\sigma(\omega) = \frac{\omega_p^2}{4\pi i \omega}[d(\omega) + g(\omega) - 1], \qquad (2)$$

where the smooth part $d(\omega) - 1$ is the response in the absence of phonons that also includes non-RPA terms. Hence the sharp structure of Eq. (2) can be written as

$$\sigma(\omega) \sim \frac{1 + D_0(\omega)[1 - \alpha']}{1 + D_0(\omega)[1 + c_1 - \alpha]}, \qquad (3)$$

where α' and c_1 are constants replacing smooth electronic responses. An explicit form for $f(\omega)$ has been derived for an incommensurate charge density wave (CDW) [21]. In this case $2\lambda\Pi_\phi(\omega) = 1 + c(\omega)$, c_1 is replaced by $c(\omega) = \frac{\lambda\omega^2}{E_r^2}f(\omega)$, and $d(\omega) = f(\omega)$ so that

$$\sigma(\omega) = \frac{\omega_p^2}{4\pi i \omega}\left\{ f(\omega)\frac{1 + D_0(\omega)[1 - \alpha]}{1 + D_0(\omega)[1 + c(\omega) - \alpha]} - 1\right\}, \qquad (4)$$

i.e., $\alpha = \alpha'$. We note that for an isolated mode either Eqs. (3) or (4) reduces to the Fano form [7].

The poles of Eq. (3), which can be found from the relation $D_0(\omega) = -(1 - \alpha + c_1)^{-1}$ (see Fig. 3), give peaks (or IRAV) in the conductivity (absorption) spectrum. On the other hand, the zeros in Eq. (3), which can be found by the relation $D_0(\omega) = -(1 - \alpha')^{-1}$ (see Fig. 3), give the indentations (or AR) in the conductivity spectrum.

To see the nonadiabatic effects on the PA spectrum we calculated the conductivity spectrum including the IRAV for polarons with low and high E_r, as seen in Fig. 4. The calculation uses the CDW form for $f(\omega)$ [21] with Eq. (4) that corresponds to a polaron charge that is sufficiently spread to form locally an incommensurate CDW; in this case E_r is the CDW gap 2Δ. For these calculations we used the phonon parameters of RR-P3HT with 13 coupled vibrational modes [22]. It is seen that when $\omega \ll E_r$, then only IRAV can be observed [Fig. 4(a)]; this happens since $c(\omega)$ in Eq. (4) is negligibly small, and consequently AR are not formed. However, when E_r is small so that the CDW band overlaps with the IRAV, then $c(\omega)$ is large so that quantum interference occurs giving rise to AR in the spectrum [Fig. 4(b)]; in this case the AR are more dominant than the IRAV that occur on their high energy side. The striking difference of the spectra for the low and
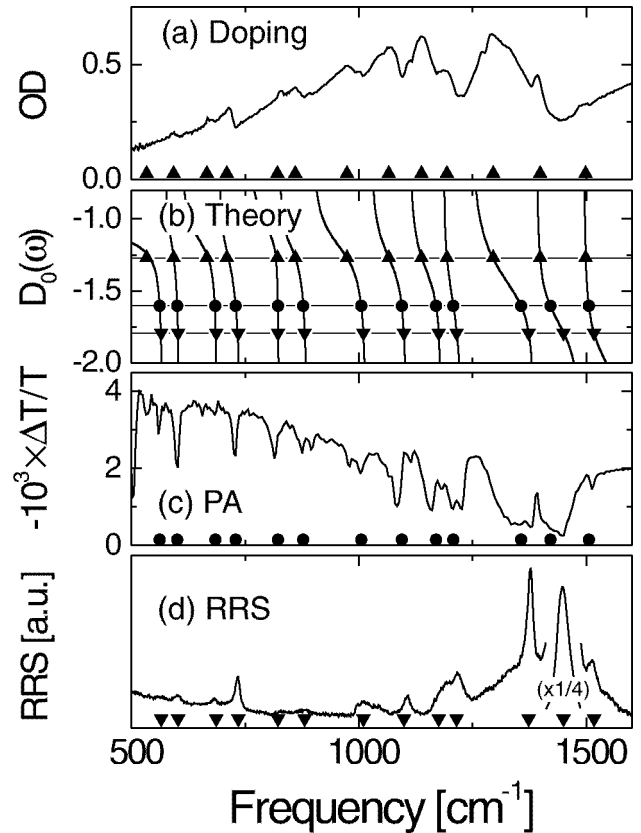

FIG. 3. The measured spectrum (lines) and calculated phonon frequencies (symbols) for (a) doping-induced absorption, (c) photoinduced absorption, and (d) resonant Raman scattering in RR-P3HT. The phonon propagator $D_0(\omega)$ is shown in (b), where the horizontal lines are obtained using $2\tilde\lambda = 0.442$ (RRS, down triangles), $\alpha' = 0.376$ (AR, circles), and $\alpha_p = 0.27$ (IRAV, up triangles).

high E_r in Fig. 4 is in agreement with the data of Fig. 1, showing that our approach captures the essence of the AR phenomenon.

To have a more quantitative fit to the experimental PA spectrum of RR-P3HT we used both RRS and doping-induced absorption spectra of this polymer film to determine the 13 bare phonon frequencies and their corresponding e-p couplings [13]. $D_0(\omega)$ based on the best fitting parameters is shown in Fig. 3(b). The 13 coupled phonons contain 12 phonons with relatively weak coupling where $\lambda < 0.1$ and a strong coupled phonon at about 2000 cm^{-1} (the C-C double bond stretching vibration) with λ_{13} of about 0.2. From these parameters we estimate a superconducting transition temperature $T_c \approx 20$ K [23]; this indicates that higher T_c may be reached in the future for RR-P3AT films with improved properties. The RRS frequencies are the solution of the equation: $D_0(\omega) = -(1 - 2\tilde\lambda)^{-1}$, where $\tilde\lambda$ is the effective e-p coupling, whereas the doping-induced IRAV frequencies are correspondingly given by the equation: $D_0(\omega) = -(1 - \alpha_p)^{-1}$, where α_p is the pinning parameter associated with the doping-induced polarons
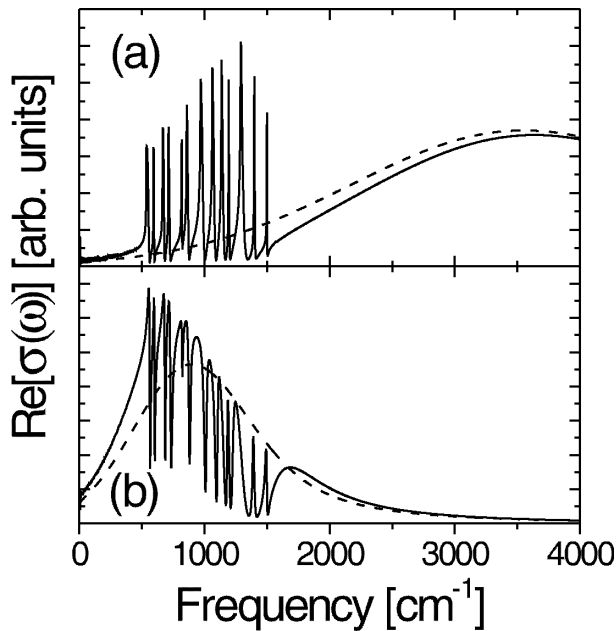
FIG. 4. Calculated PA spectra (solid lines) using the CDW response function $f(\omega)$ (broken lines) with onset 2Δ at (a) $2\Delta = 3600$ cm^{-1} and FWHM of 2400 cm^{-1}, (b) $2\Delta = 800$ cm^{-1} and FWHM of 800 cm^{-1}.

[13]. The obtained bare phonon parameters for RR-P3HT [22] were used to calculate, via the AM model, the doping-induced IRAV, RRS, and AR frequencies as seen in Figs. 3(a), 3(c), and 3(d).

The actual fit to the RR-P3HT photoinduced AR spectrum is seen in Fig. 2(f) and can be compared with the measured spectrum [Fig. 2(e)]. The excellent agreement between theory and experiment was obtained by using Eq. (4) with the above AM parameters together with the CDW absorption band [21] representing the polaron P_1 band with $2\Delta = 800$ cm^{-1}. For this fit a distribution in 2Δ of 100% and a distribution in α of about 33% around $\alpha = 0.376$, with $c_1 = -0.08$ was necessary. The disorder and inhomogeneity that still exist in RR-P3HT films in spite of the lamella formation justify the parameter distributions.

In view of the excellent agreement between theory and experiment that is seen in Figs. 2(e) and 2(f) and the close correspondence of Figs. 1 and 4, we conjecture that the AM model and a continuum electronic band such as the CDW can quantitatively describe the AR phenomenon in ordered PCP films. This conclusion strongly indicates that the photoinduced polaron band in such materials is continuous and, consequently, the electronic band above the localized polaron level in the gap is also continuous.

We thank K. Yoshino for the PDPA and PFO samples, Y. Okamato for the PPE sample, U. Sherf and K. Müllen

[1] R. H. Friend et al., Nature (London) 397, 121 (1999).
[2] H. Sirringhaus et al., Nature (London) 401, 685 (1999).
[3] R. Österbacka, C. P. An, X. M. Jiang, and Z. V. Vardeny, Science 287, 839 (2000).
[4] H. Sirringhaus, N. Tessler, and R. Friend, Science 280, 1741 (1998); B. Crone et al., Nature (London) 403, 521 (2000).
[5] J. H. Schön et al., Nature (London) 410, 189 (2001).
[6] L. Sebastian and G. Weiser, Phys. Rev. Lett. 46, 1156 (1981).
[7] B. Horovitz, Solid State Commun. 41, 729 (1982).
[8] F. L. Pratt, K. S. Wong, W. Hayes, and D. Bloor, J. Phys. C 20, L41 (1987); J. Phys. D 20, 1361 (1987).
[9] Y. H. Kim, D. Spiegel, S. Hotta, and A. J. Heeger, Phys. Rev. B 38, 5490 (1988).
[10] D. Comoretto et al., Phys. Rev. B 49, 8059 (1994).
[11] H. Johanson et al., Synth. Met. 101, 192 (1999).
[12] P. J. Brown, H. Sirringhaus, M. Harrison, M. Shkunov, and R. H. Friend, Phys. Rev. B 63, 125204 (2001).
[13] E. Ehrenfreund, Z. Vardeny, O. Brafman, and B. Horovitz, Phys. Rev. B 36, 1535 (1987).
[14] M. J. Rice, Phys. Rev. Lett. 37, 36 (1976).
[15] B. Horovitz, H. Gutfreund, and M. Weger, Phys. Rev. B 17, 2796 (1978).
[16] U. Fano, Phys. Rev. 124, 1866 (1961).
[17] F. Cerdeira, T. A. Fjeldly, and M. Cardona, Phys. Rev. B 8, 4734 (1973).
[18] M. V. Klein, in Light Scattering in Solids, I, edited by M. Cardona (Springer, Heidelberg, 1983), p. 147.
[19] S. Glutsch, U. Siegner, M. A. Mycek, and D. S. Chemla, Phys. Rev. B 50, 17 009 (1994).
[20] V. I. Belitsky et al., J. Phys. Condens. Matter 9, 5965 (1997).
[21] For CDWs the gap is $E_r = 2\Delta$; we have when $\omega < 2\Delta$ that $f(\omega) = \frac{4\Delta^2}{\omega^2 y}\arctan(1/y)$ while when $\omega > 2\Delta$ $f(\omega) = \frac{2\Delta^2}{\omega^2 y}[\ln(\frac{1-y}{1+y}) + \pi i]$, where $y = \sqrt{|1 - 4\Delta^2/\omega^2|}$.
[22] Most of the bare frequencies are very close to the extrapolated vertical lines in Fig. 3(b), with an average coupling $\lambda_n/\lambda = 0.007$. The five most important modes have the following frequencies (in cm^{-1}) and couplings: $\omega_{13} = 1996$, $\lambda_{13}/\lambda = 0.876$; $\omega_{10} = 1237$, $\lambda_{10}/\lambda = 0.019$; $\omega_7 = 1020$, $\lambda_7/\lambda = 0.011$; $\omega_6 = 890$, $\lambda_6/\lambda = 0.014$; $\omega_4 = 745$, $\lambda_4/\lambda = 0.024$.
[23] B. Horovitz, Phys. Rev. B 16, 3943 (1977).